Separation and Purification Technology 313 (2023) 123475

Contents lists available at ScienceDirect

Separation and Purification Technology

journal homepage: www.elsevier.com/locate/seppur

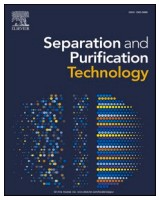

Molecular thermodynamic model for solvent extraction of mineral acids by tri-*n*-butyl phosphate (TBP)

Rayco Lommelen [a,*], Koen Binnemans [a]

[a] KU Leuven, Department of Chemistry, Celestijnenlaan 200F, P.O. Box 2404, B-3001 Leuven, Belgium

ARTICLE INFO

Keywords:
Acids
Chemical thermodynamics
Liquid–liquid equilibria
Mixed-solvent electrolyte model
Solvent extraction

ABSTRACT

Removal or recovery of acids by solvent extraction is highly relevant for recycling, process control, and wastewater decontamination, especially in the hydrometallurgical industry. The construction and optimization of such processes would benefit from a molecular thermodynamic model that can predict liquid–liquid equilibria. Past attempts resulted in models that were not very predictive. Therefore, a new approach was followed and demonstrated for the extraction of the mineral acids (inorganic acids) HNO_3, HCl, H_2SO_4, H_3PO_4, and H_3AsO_4 by tri–*n*–butyl phosphate (TBP). The semi-empirical OLI Mixed-Solvent Electrolyte (MSE) framework was used to construct the thermodynamic model for calculating the liquid–liquid equilibria. Contrary to previous attempts, this framework allows the description of both the aqueous and organic phases in one model, and it can accurately deal with the non-ideal behavior of concentrated electrolyte solutions. The best agreement between calculated and experimental distribution data was achieved by assuming that the extraction of mineral acids occurs via protonation of TBP and coextraction of the anions. At very high acid concentrations, also neutral acid molecules are transferred to the organic phase. The high accuracy of the thermodynamic model for all mineral acid systems considered in this study is an indication that this approach for modeling liquid–liquid equilibria is a universal one. Furthermore, the extraction of mineral acids can be predicted in mixed-acid systems and acid-salt systems that were not used to construct the model.

1. Introduction

Recovery of acids from aqueous streams is essential in a broad range of chemical and metallurgical processes. Examples include acid removal from waste solutions to manage environmental concerns, acid recycling to lower the consumption of chemicals, and acidity control during or in between unit operations [1–3]. Solvent extraction is an interesting technique for acid recovery. It avoids the large chemical consumption and waste generation typical for the neutralization of acids by addition of alkali.

Many chemical reactions occur in a single solvent extraction process, often at conditions far from thermodynamic ideality when electrolytes are involved [4,5]. Usually, several moles of acid per liter are dissolved in an aqueous phase that also contains significant quantities of inorganic salts or organic molecules. This complex aqueous phase is then contacted with an organic phase containing an extractant, a diluent, and sometimes a modifier. The interaction of the acid and other species with the extractant, and the solvation of the resulting species by the diluent only add to the complexity of the system. The modifier is used to fine-tune the solvent extraction process and to avoid third-phase formation, but it also further increases the complexity.

Because of this complexity, solvent extraction processes require careful optimization of a large number of process variables [6]. It is also difficult to predict the effects of changes in these variables on the liquid–liquid equilibria and the distribution ratios, due to the large deviations from thermodynamic ideality in the aqueous and organic phases. This leaves a large degree of freedom to design optimal solvent extraction processes, but it also leads to a time-consuming trial-and-error approach to finding the optimum conditions.

Computational modeling can significantly reduce the time required for the design and optimization of solvent extraction processes, including extraction processes for acids [7]. Such computational models become more useful if they are predictive, i.e. when they can predict the behavior of a system outside the range of conditions used to construct them [8]. This makes the model more broadly applicable and improves its reliability. There exist already a few computational models to calculate solvent extraction involving electrolyte solutions, but these are based on mathematical or chemical frameworks that have limited

* Corresponding author.
E-mail address: rayco.lommelen@kuleuven.be (R. Lommelen).

https://doi.org/10.1016/j.seppur.2023.123475
Received 26 January 2023; Received in revised form 23 February 2023; Accepted 23 February 2023
Available online 28 February 2023

predictive power [9–17]. Most of these models have been developed by the nuclear industry, to model the reprocessing of spent nuclear fuel, such as the PUREX process.

The simplest models are completely empirical, in the sense that parametric mathematical functions are fitted to the experimental distribution isotherms. These models ignore any underlying chemistry and hence have no predictive power. The simplest chemical models rely on a set of reaction equations with equilibrium constants to describe a solvent extraction process. Here, fictitious chemical species are necessary to describe processes that occur far from thermodynamic ideality. By working in a chemical model with activities rather than concentrations, the need to introduce fictitious species is avoided, but it is extremely difficult to rigorously calculate the activity of a species at highly non-ideal conditions. These activity equations are typically semi-empirical [18]. They have a sound chemical basis, but they also contain parameters that must be determined by fitting the activity equations to experimental data such as water vapor pressures. The available solvent extraction models that use activity equations still have limited predictability because a thermodynamic framework is used that cannot describe the whole solvent extraction process. For instance, several publications report a thermodynamic framework with activity equations to describe the aqueous phase, but they assume ideal thermodynamic behavior of the organic phase [9–11,17]. This assumption is not correct when high extractant concentrations are used or when the organic phase is highly loaded with acids or other electrolytes.

There exist also purely theoretical models, such as COSMO-RS [19]. Although these are highly predictive and they do not require any empirically determined parameters, they cannot (yet) calculate a complete solvent extraction process [6]. The chemical species and interactions between these species are too complex for the current computational methods to converge in a reasonable amount of time.

To get a predictive model that can reliably calculate liquid–liquid equilibria relevant to solvent extraction of acids, we constructed a semi-empirical model based on the OLI Mixed-Solvent Electrolyte (OLI-MSE) thermodynamic framework [20,21]. Hereby, one consistent thermodynamic framework is used to describe the whole solvent extraction process for all compositional varieties of the modeled chemical system. In this paper, we demonstrate that this model can accurately calculate and predict the solvent extraction of HNO_3, HCl, H_2SO_4, H_3PO_4, and H_3AsO_4 by the neutral extractant tri-*n*-butyl phosphate (TBP), without the need for introducing fictitious chemical species in the model. For this modeling approach, we chose TBP as the extractant because it is a well-known compound, often used in solvent extraction processes [6]. The mineral acids were chosen to test whether our approach is generic and can be applied to more than one acid because these mineral acids make up the bulk of mineral acids used in relevant processes. H_3AsO_4 extraction by TBP is relevant for, for instance, the removal of toxic arsenic from copper refinery electrolytes [22]. The research presented here also aims to provide better tools to develop these new solvent extraction processes and to get insights into the molecular mechanisms behind them [23–26].

2. Model description

2.1. Thermodynamic framework

The OLI Mixed-Solvent Electrolyte (OLI-MSE) thermodynamic framework version 11.0 of OLI Systems Inc. (Parsippany NJ) was chosen to model the solvent extraction of acids using the OLI Studio 11, OLI Databook 11, and OLI Chemistry Wizard 11 software packages of OLI Systems Inc. (Parsippany NJ). These are commercial software packages that allow users to build their own thermodynamic model and database. The thermodynamic framework can describe the behavior of electrolytes and non-electrolytes in mixed-solvent systems (mixtures of aqueous and organic solvents) [20,21]. Thus, it is suited to calculate the complete liquid–liquid equilibrium (LLE) that describes the solvent extraction process of acids by TBP. The OLI-MSE framework achieves this by combining speciation-based standard-state thermodynamic properties (like the standard-state Gibbs energy (G^0) with extensive activity-coefficient equations to account for physical interactions between molecules. The *excess Gibbs energy* (G^{EX}) is used for the activity equations:

$$\frac{G^{EX}}{RT} = \frac{G^{EX}_{SR}}{RT} + \frac{G^{EX}_{MR}}{RT} + \frac{G^{EX}_{LR}}{RT} \quad (1)$$

This expression is divided into a short-range (SR), a mid-range (MD), and a long-range (LR) contribution, and R and T are the gas constant and temperature, respectively.

The local-composition-based *Universal Quasi-Chemical* (UNIQUAC) framework is used for the short-range contributions [27]. It requires only binary interaction parameters between species i and j (a_{ij} and a_{ji}), a surface parameter (q_i) and a size parameter (r_i). The UNIQUAC framework is appropriate to model complex phase equilibria because it captures both intermolecular forces and entropic contributions, and only a limited number of adjustable parameters are required [18]. Further extension of G^{EX} with mid-range and long-range contributions is necessary to model solvent extractions of acids because the UNIQUAC framework cannot deal with electrolytes.

The long-range electrostatic interactions enable to describe electrolyte chemistry of dilute to semi-concentrated solutions (up to 6 molal). These interactions are calculated in the OLI-MSE framework by a Pitzer extension of the Debye-Hückel equation (modified Pitzer–Debye–Hückel equation) [20]. No interaction parameters are necessary for the long-range contribution as it only depends on the charges in the solution surrounding the ion in question and on the dielectric constant of the solution. The charge of a solute is entered directly into the OLI database, and the dielectric constant of any solution is estimated by a general model that uses the pure components' dielectric constants [20,28]. The dielectric constants of the solvents are already available in the general OLI database. Therefore, the long-range interactions are calculated automatically, and they are not further discussed in this paper.

The long-range and short-range interactions do not suffice when calculating concentrated electrolyte solutions (above 6 molal) and overly complex systems. To solve this problem, mid-range contributions are introduced. It is a symmetrical second virial coefficient-type equation that resembles the approach to account for deviations from the ideal gas law in the gas phase [20]. The mid-range equations use an ionic-strength-independent binary interaction parameter (b) and an ionic-strength-dependent binary interaction parameter (c) to describe ion/ion and ion/neutral interactions at high ionic strengths.

All these binary interaction parameters, and, if necessary, also the G^0 or other standard-state thermodynamic values, can be determined by fitting the activity-coefficient equations to experimental data via regression procedures. The OLI regression tool was used for this work. These data ideally reflect directly the activity of every species in all relevant binary mixtures, but this is impractical or even impossible for most species. To model solvent extraction, data about the speciation of species in a phase, water activity data, and distribution data for every species should thus suffice. The experimental data used to construct the thermodynamic model are always data at room temperature unless otherwise stated.

To obtain a consistent thermodynamic framework, which is essential for calculating the LLE, the OLI-MSE framework uses the symmetrical reference state internally for its standard state and excess contributions. It also assures that the *chemical potential* of a species (μ_i) is equal in every phase [21]. This is the basis for LLE equilibria. By requiring equal μ_i in two liquid phases (α and β) at equilibrium and calculating the activity coefficient (γ_i) of that species i in every phase, the distribution of that species between both liquid phases is found as the mole fraction of that species (x_i) in both phases:

$$\mu_i^{\alpha} = \mu_i^{\beta} \quad (2)$$

$$\mu_i^{\alpha} = \mu_i^0 + RT\ln(x_i^{\alpha}\gamma_i^{\alpha}) \quad (3)$$

And then by substituting (3) in (2)

$$\mu_i^0 + RT\ln\left(x_i^{\alpha}\gamma_i^{\alpha}\right) = \mu_i^0 + RT\ln(x_i^{\beta}\gamma_i^{\beta}) \quad (4)$$

$$x_i^{\alpha}\gamma_i^{\alpha} = x_i^{\beta}\gamma_i^{\beta} \quad (5)$$

Although the OLI-MSE framework is designed to calculate mixed-solvent systems and electrolyte solutions, it is not able to completely calculate all chemical processes relevant to all types of solvent extractions [29]. More particularly, this framework can calculate only equilibria in homogeneous phases, but some extractants aggregate in the organic phase under certain conditions to form inverse micelles or microemulsions. An OLI-MSE-based solvent extraction model of a system where these aggregates are formed, and where the aggregates significantly influence the solvent extraction process will thus give less reliable results [30]. For the presented acid–TBP model, and for many other solvent extraction systems, such problems do not arise. Furthermore, the OLI-MSE framework was chosen to create a solvent extraction model of acids by TBP because no other framework was identified that can calculate simultaneously the complex electrolyte solution chemistry, mixed-solvent systems, and aggregation. It is also easily accessible and applicable for the calculation of multistage solvent extraction processes with, for instance, flowsheet simulators. The OLI-MSE framework uses UNIQUAC interaction parameters for the short-range contributions, which is preferred over the (e)NRTL framework when calculating solvent extraction. The (e)NRTL framework is not very successful in describing larger molecules, like extractants, because it is more suited for the calculation of the excess enthalpy rather than the excess Gibbs energy [18]. There were some attempts to unify the short-range coordination and solvation chemistry with long-range aggregation interaction into a thermodynamic model, but these require further development before they can be used accessibly on a large variety of systems [31,32].

2.2. Chemical model

There are several experimental and modeling studies available on the extraction mechanism of mineral acids by TBP [3,10–12,33–38]. Traditionally, any deviation of the experimental or calculated data from a concentration line predicted by the formation of one acid–extractant complex was mitigated by the introduction of another acid–extractant complex in the chemical model. Often there was no experimental evidence for the existence of the postulated species, nor were these predicted by means of computational chemistry. Without any experimental or theoretical evidence, it is difficult to justify adding several extra species to the model. The deviations often disappear if calculations are done by considering activities rather than concentrations of the species. Different speciation studies often give contradictory results about the concentration ranges in which a certain species is the dominant one. This is especially true at the high acid concentrations that are relevant for the solvent extraction of these acids. At these high concentrations, significant deviations from ideal thermodynamic behavior are expected that require the use of the activities rather than concentrations in both the aqueous and organic phase to account for all types of physicochemical interactions between the acids, extractants, and their surroundings. Unfortunately, it is not easy and often even not possible to directly measure the activity of a species in a complex solution.

The OLI-MSE thermodynamic framework can accurately calculate the activity of the species involved in the extraction process. This avoids the need to introduce fictitious species. Therefore, the number of chemical species required to accurately calculate the liquid–liquid equilibria of acids can be kept at a minimum.

Because TBP is a weak Brønsted base, the phosphate oxygen atom of TBP can bind a proton to form the protonated species $TBPH^+$ [39,40]. Literature data suggest a $pK_a < 0$ for $TBPH^+$, and hence, protonation of TBP occurs only at high proton activities [41,42]. An accurate estimation of the pK_a value of $TBPH^+$ at thermodynamic ideal conditions is required to calculate the formation energy of $TBPH^+$ from that of TBP. However, the determination of a sufficiently accurate pK_a value of $TBPH^+$ at standard conditions is difficult because high concentrations of reagents are necessary to protonate TBP. Furthermore, the pK_a will vary depending on the solvent that surrounds TBP. A pK_a value of −0.5 was used, as a reasonable estimate, as the initial value of the formation energy of $TBPH^+$ in the thermodynamic model we present. Weak acids will not protonate TBP. In that case, the acid can still be extracted as a neutral molecular compound by only weakly interacting with the phosphoryl oxygen atom of TBP.

Depending on the acid, a larger or smaller fraction of it will be extracted by proton transfer. The complete extraction mechanism then becomes:

$$HX + \overline{TBP} \rightleftharpoons \overline{TBPH^+} + \overline{X^-} \quad (6)$$

$$HX \rightleftharpoons \overline{HX} \quad (7)$$

Here, HX depicts a mineral acid, and the overbar denotes a species in the organic phase. This extraction mechanism is a universal one for any acid. To assess the feasibility of this extraction mechanism, the extraction of three different strong acids (HNO_3, HCl, and H_2SO_4) and two weak acids (H_3PO_4 and H_3AsO_4) were modeled. It should be possible to model the extraction of all these acids by optimizing the behavior of $TBPH^+$, while also fine-tuning the extraction efficiency of the neutral HX species and the water uptake of the organic phase by adjusting the interaction between the coextracted anion (X^-) or acid molecule (HX) and the extractant.

3. Results and discussion

The overall method to build the thermodynamic model is schematically represented in Fig. 1. This is a general workflow that can be applied to model complex systems with the OLI-MSE thermodynamic framework using the OLI software packages. A more in-depth discussion of all steps in this flowchart is given throughout the results and discussion section. This detailed discussion is combined with a presentation and discussion of the modelling results because the exact contents of a modelling step in the flowchart are determined by the results of the previous step and *vice versa*. This is also evident from the feedback loops built into the flowchart.

3.1. Standard-state thermodynamics

The standard-state thermodynamic values and UNIQUAC surface (q) and size (r) parameters of TBP were already available in the OLI-MSE database (Table 1). These were used as a starting point for the construction of the thermodynamic model. The standard-state Gibbs formation energy (ΔG_f^0) of $TBPH^+$ was calculated based on its estimated pK_a value and the ΔG_f^0 of TBP, H_2O and H_3O^+ (Table 1). This value for $TPBH^+$ was kept constant during the construction of the model while the interaction parameters of $TBPH^+$ with the other species were optimized.

The initial value for the standard-state entropy (S^0) of $TBPH^+$ was estimated by adding the entropy of H_3O^+ to that of TBP and subtracting the entropy of H_2O. This gave only a rough estimate that was further optimized during the construction of the complete model to achieve an accurate calculation of the temperature dependence of the extraction of the acids between 20 °C and 60 °C.

The standard-state enthalpy of formation (ΔH_f^0) of $TBPH^+$ was then determined as follows:

$$\Delta H^0_{f,TBPH^+} = \Delta G^0_{f,TBPH^+} + T\left(S^0_{TBPH^+} - \sum S^0_{elements}\right) \quad (8)$$

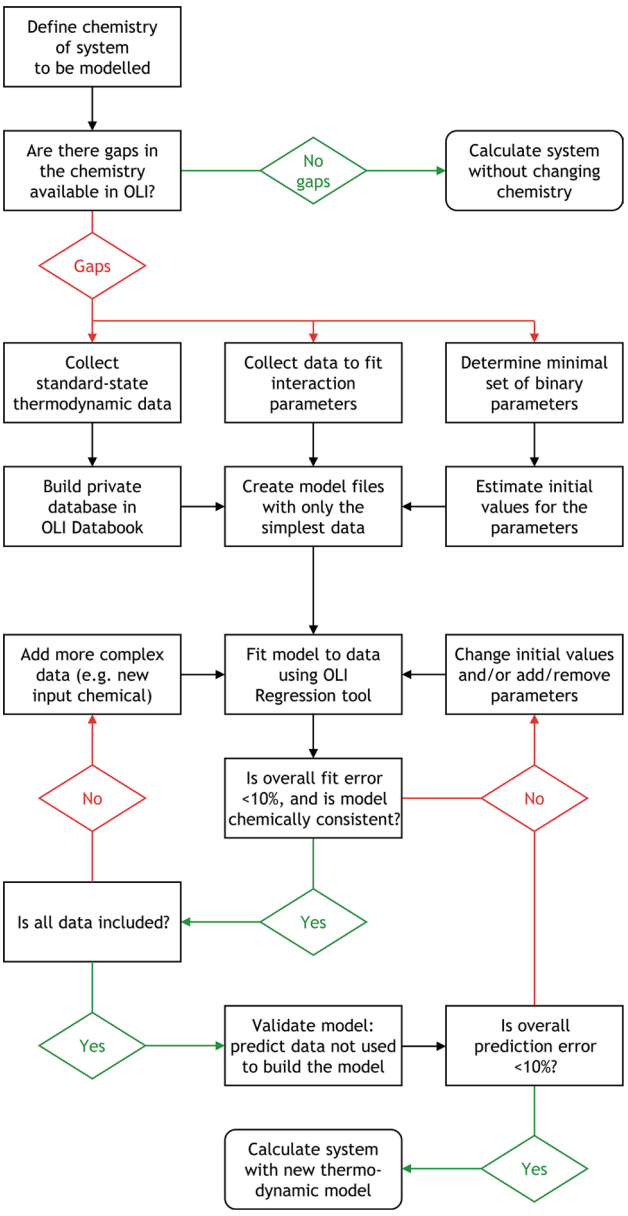

Fig. 1. High-level flowchart on how to build a thermodynamic model for a complex chemical system using the OLI-MSE framework and the OLI software packages.

Table 1
Standard-state thermodynamic properties and UNIQUAC surface and size parameters of TBP, H_2O, H_3O^+, and $TBPH^+$. The values for TBP, H_2O, and H_3O are taken from OLI Systems, while these of $TBPH^+$ are the optimized values in the thermodynamic model.

Species	ΔG_f^0 (kJ mol^{-1})	ΔH_f^0 (kJ mol^{-1})	S_f^0 (J mol K^{-1})	v^0 (L mol^{-1})	q	r
TBP	−812.9	−1423.4	234.7	0.272	14.82	11.85
H_2O	−237.3		103.4			
H_3O^+	−274.3		70.04			
$TBPH^+$	−800.1	−1380.7	400.1	0.272	2.685	3.366

This ΔH_f^0 was treated as a constant with respect to temperature, because temperature effects were limited in the investigated temperature range.

The UNIQUAC surface (q) and size (r) parameters of $TBPH^+$ were allowed to change during the construction of the model to find an optimal fit between the calculated and all available experimental data. The final values of the UNIQUAC surface and size parameters (Table 1) deviate significantly from the initial values of TBP but are closer to the typical values for ions in the OLI-MSE framework ($q = 0.92$ and $r = 1.4$).

Also, molar volumes (v^0) of every pure liquid are required in the OLI-MSE framework to help with the conversion of mole fraction or mole-based quantities in volumes and volumetric concentrations. This is specifically important for the calculation of solvent extraction data because these are almost always depicted in volumetric concentrations. Contrary, the OLI-MSE framework uses mole fraction internally and the experimental data used to determine the interaction parameters by data fitting should be added in units of moles.

3.2. Water and extractant solubility

Interaction parameters between TBP/$TBPH^+$ and their surroundings are required to accurately calculate the activity coefficients of all species in the biphasic solvent extraction system because the LLE is calculated based on the differences in activity coefficients of a species in both liquid phases. Before the extraction of acids can be calculated, the LLE between extractant and water should be added to the thermodynamic model. This was done by fitting the UNIQUAC binary interaction parameters of TBP and water to experimental solubility data of water in TBP and of TBP in water (Fig. 2 and Fig. 3) [35,43]. The resulting interaction parameters of this and other regressions are summarized in Table 2.

The data of Colón *et al.* give the solubility of water in organic phases from low to high TBP concentration [35]. *n*-Dodecane is used as the diluent. At the start of the optimization procedure, no interaction parameters between TBP and *n*-dodecane are needed, because only binary interaction parameters between species and the measured property in the experiment are necessary. The UNIQUAC binary interaction parameters between *n*-dodecane and water were already available in the OLI-MSE database, so only interaction parameters between TBP and water were added to calculate the LLE for the systems comprising water and (un)diluted TBP.

From the data of Velavendan *et al.*, only the data points without acid were modeled to initialize the LLE calculations of TBP and water [43]. The other data points with acid can only be used for the regression of interaction parameters together with all other relevant data for these systems. Thus, the data points with acids can only be used once the extraction of acid is optimized by also including acid extraction data. Other binary interaction parameters should also be taken into account for that optimization. For instance, these are the parameters representing the physicochemical interactions between $TBPH^+$ and water.

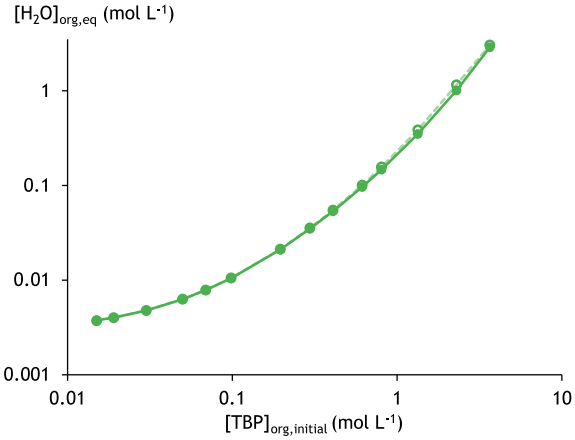

Fig. 2. Final model fit (filled markers) to experimental data for the solubility of water in TBP diluted in *n*-dodecane (open markers). Experimental data from Colón et al. [35].

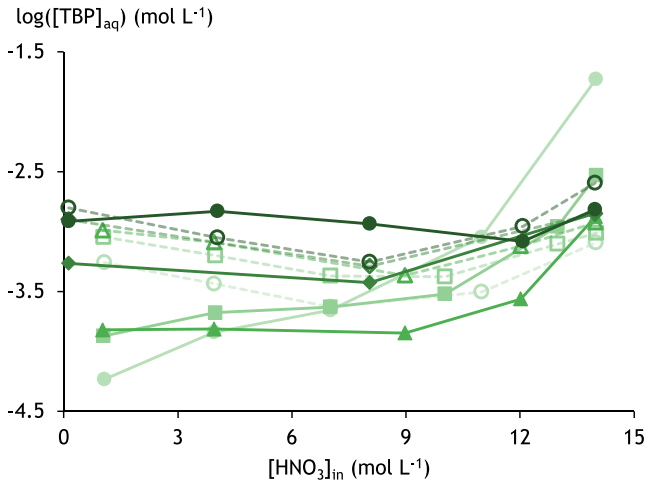

Fig. 3. Final model fit (filled markers) to experimental data of aqueous solubility of TBP (open markers) from Velavendan et al. [43]. $[TBP]_{initial}$ increases from light to dark green as follows: 5 vol% (●), 20 vol% (■), 1.1 mol L^{-1} (▲), 65 vol% (◆), undiluted TBP (●).

Table 2
Optimized UNIQUAC and MIDRANGE binary interaction parameters for the extraction of HX by TBP.

Species	UNIQUAC[a]		MIDRANGE[b]	
	a_{ij}	a_{ji}	b_{ij}	c_{ij}
H_2O–TBP (0)[c]	−10695	6822.3		
H_2O–TBP (1)[c]	71.123	−36.089		
H_2O–TBP (2)[c]	−0.10391	0.076991		
H_2O–$TBPH^+$	11,699	3634.7		
n-dodecane–TBP	−2267.9	1768.8		
n-dodecane–$TBPH^+$	5432.0	−5762.2		
TBP–H_3O^+			−8.9536	
$TBPH^+$–H_3O^+			−25.528	
$TBPH^+$–HNO_3	−6649.0		12.739	−18.587
TBP–HCl	−12714			
$TBPH^+$–HCl			2.000	
TBP–Cl^-			−6.8515	
$TBPH^+$–Cl^-			−5.8180	
TBP–HSO_4^-			−5.8593	
$TBPH^+$–HSO_4^-			−12.925	
TBP–SO_4^{2-}			−10.000	
$TBPH^+$–SO_4^{2-}			−10.000	
TBP–H_3PO_4 (0)[d]		4921.5	−19.769	
TBP–H_3PO_4 (2)[d]			7217.0	
$TBPH^+$–H_3PO_4		6443.3	3.6487	
TBP–$H2PO_4^-$			−2.9429	
$TBPH^+$–$H2PO_4^-$			1.7381	
TBP–Ca^{2+} (2)[d]			−7500	
n-dodecane–HSO_4^- (2)[d]			−4583.23	

[a] short-range binary interaction parameters.
[b] mid-range binary interaction parameters: $MR(ij) = b_{ij} + c_{ij} \bullet exp\left(-\sqrt{I+0.01}\right)$ with *I* the ionic strength of the solution.
[c] $a_{ij} = a(0)_{ij} + a(1)_{ij} \bullet T + a(2)_{ij} \bullet T^2$ with *T* the absolute temperature in Kelvin.
[d] $b_{ij} = b(0)_{ij} + b(2)_{ij}/T$

3.3. Single acid extraction by undiluted TBP

From the moment that acid is present in the system, the extraction of acid should be included in the construction of the model. From this point on, also the protonation of TBP should be optimized together with the distribution ratio of $TBPH^+$ between the aqueous and organic phases. The anions of the mineral acids are coextracted and their interactions with the extractant and the diluent can be described in the model using interaction parameters. At the highest acid concentrations and for weak acids, significant amounts of undissociated acid molecules are present and they will also distribute between the organic phase and the aqueous phase. Hence, interaction parameters between the extractant and the undissociated acid molecules should be included as well.

Note that it was not necessary to determine the behavior of the acids in the aqueous phase because OLI Systems already extensively optimized acids in water. For instance, OLI researchers have published a paper that describes the H_2SO_4 system for the whole concentration range from 0 % to 100 % H_2SO_4 [21]. Similarly, the solubility of H_2O and the acids in common diluents has already been added to the OLI-MSE database by OLI systems. The only change necessary here was the optimization of the *n*-dodecane – HSO_4^- MIDRANGE interaction parameter to get a higher solubility of the lower charged HSO_4^- species in the organic phase compared to SO_4^{2-} (Table 2).

First, only data from systems with undiluted TBP and a single mineral acid were added to the regression to limit the complexity of the parameter optimization. These include the extraction of HNO_3, HCl, H_2SO_4, and H_3PO_4. A combination of literature sources was used to collect the data necessary to build the thermodynamic model. The thermodynamic model can accurately calculate the extraction of the four investigated acids by undiluted TBP under the conditions described above (Fig. 4a). Experimental data came from Hanson and Patel [37], Peppard *et al.* [34], Hanson and Patel [37], Kertes [34], Hesford and McKay [33], Ziat *et al* [44], Dhouib-Shanoun *et al.* [45], and Zhang *et al.* [46]. To fully characterize the composition of both phases of the LLE,

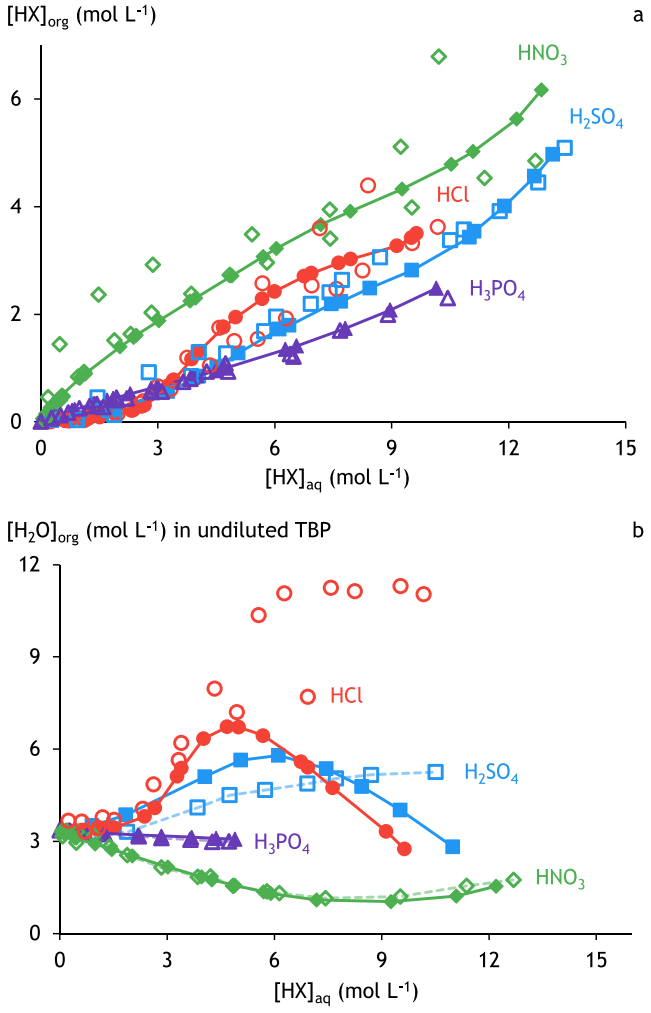

Fig. 4. Final model fit (filled markers and lines) to experimental data (open markers) of (a) acid extraction and (b) the solubility of water in the organic phase [13,33,34,37,44–47]. HX is HNO_3 (◊), HCl (○), H_2SO_4 (□), or H_3PO_4 (Δ).

also the solubility of water in undiluted TBP was fitted (Fig. 4b). Relevant experimental data were taken from Puzikov *et al.* [11], Hesford and McKay [33], Kertes [34], and Ziat *et al.* [44].

The basis for the calculation of the acid extraction is the protonation of TBP with coextraction of the anions of the acids for all four acids. An accurate calculation of the distribution of water, TBP and $TBPH^+$ between the aqueous and organic phases is obtained by optimizing the UNIQUAC binary interaction parameters between water and TBP/$TBPH^+$ (Table 2). MIDRANGE binary interaction parameters between H_3O^+ and TBP/$TBPH^+$ were used to further fine-tune the system.

A large part of the experimental differences between acid and water extraction in the different systems can be explained by differences in acid hydration and by the different pK_a values of the acids. These differences between the four acid systems arise in the thermodynamic model because of the correct calculation of the acid and water activity, and because of the accurate calculation of the deprotonation equilibria of the mineral acids. No changes were made in this regard to the thermodynamic model because the aqueous phase behavior is already accurately added to the OLI-MSE database by OLI systems (*vide supra*). The OLI-MSE thermodynamic model was optimized further by introducing binary interaction parameters between the specific mineral acids and TBP/$TBPH^+$ (Table 2). This was necessary to account for the non-covalent interactions of the acids with the extractant in the organic phase, which explain the remaining differences in acid and water extraction. An overview of the calculated speciation in the organic phase is given in Fig. 5. This calculation is chemically logical, with only the formation of undissociated inorganic acid molecules at the highest acid concentrations for the strong acids, and it follows the order of the pK_a values of the mineral acids in the aqueous phase [48]. As expected, the weak acid H_3PO_4 is extracted predominantly as the undissociated acid in the thermodynamic model.

Note that the number of adjustable binary interaction parameters is kept to a minimum that still accurately reflects the experimental data. This approach is followed to reduce the risk of overfitting. The differences between the fit and experimental data of the concentration of $[H_2O]_{org}$ (Fig. 4b) could not be improved by introducing more binary interaction parameters. First, the discrepancy of $[H_2O]_{org}$ in the HCl system arises from experimental errors. The data from Kertes (high $[H_2O]_{org}$) do not match with those of Hesford and McKay. It was not possible to verify which experimental dataset is correct, or whether both are inaccurate. Secondly, the drop in $[H_2O]_{org}$ calculated by the thermodynamic model at very high acid concentrations is not reflected in the experimental data. The lowered $[H_2O]_{org}$ in the calculations might be explained by a very low calculated water activity at these data points (0.05–0.3). This suggests that almost no water is present under these conditions and the water that is present is significantly less *free*. The available water molecules strongly interact with the acid, which is also available in very large quantities.

No significant amounts of $TBPH^+$ are formed when H_3PO_4 is extracted from aqueous solutions that contain only H_3PO_4. Nevertheless, it is important to determine the relevant binary interaction parameters between phosphoric acid species and $TBPH^+$ for the calculation of H_3PO_4 extraction in mixed-acid systems. To determine these interaction parameters, a dataset for the extraction of H_2SO_4 and H_3PO_4 from mixed acid aqueous solutions was added [49]. The extraction of H_2SO_4 is calculated quite accurately (Fig. 6a), even without optimization of binary interaction parameters that contain H_2SO_4 or its deprotonated species. The fit for the extraction of H_3PO_4 can be found in Fig. 6b. It was combined with the previous datasets that contain H_3PO_4 to finetune the relevant binary interaction parameters (Table 2).

In general, extractants are used in diluted form rather than in undiluted form. Mixing the extractant with a non-reactive diluent might improve the physicochemical properties of an extraction system and the extractant concentration can be used as an extra variable to optimize the selectivity and extraction power of the extraction system [6]. Therefore, the extractant concentration and diluent effects were added to the thermodynamic model. Long-chain aliphatic organic solvents are frequently used to dilute TBP [33,50]. *n*-Dodecane was used as a model

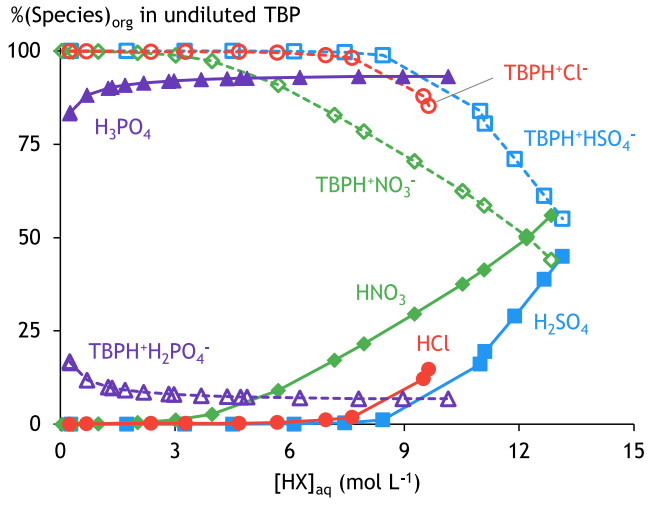

Fig. 5. Speciation of the extracted acids, as calculated by the MSE-OLI model. HX is HNO_3 (◆), HCl (●), H_2SO_4 (■), or H_3PO_4 (▲).

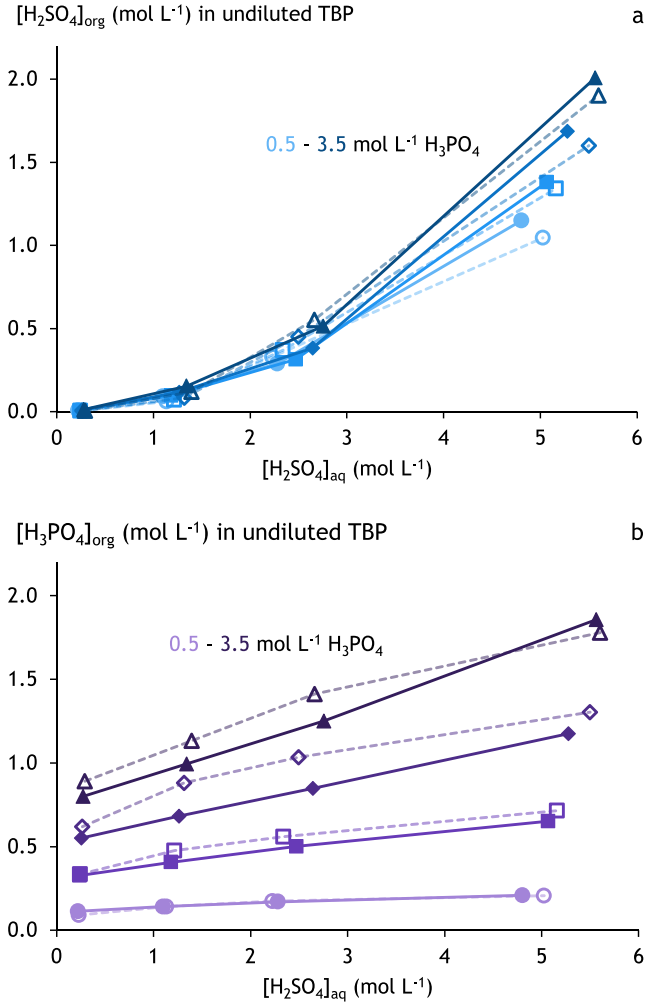

Fig. 6. Model fit (filled markers) to experimental data of the extraction of (a) H_2SO_4, and (b) H_3PO_4 from mixed acid solutions (open markers) [49]. The labels show the initial H_3PO_4 concentrations: 0.5 mol^{-1} (●), 1.5 mol^{-1} (■), 2.5 mol^{-1} (◆), and 3.5 mol^{-1} (▲).

diluent in the thermodynamic model for these types of diluents because the differences between different diluents on the solvent extraction system are usually small [51].

More specifically, UNIQUAC interaction parameters between *n*-dodecane and TBP/$TBPH^+$ were determined by fitting the thermodynamic model to experimental data on the extraction of HNO_3, H_2SO_4, and H_3PO_4 (Fig. 7a and Fig. 8) [33,35–37,45,47,50]. The solubility of water in the organic phases of the HNO_3 – TBP extraction systems was also optimized during the optimization of the binary interaction parameters (Fig. 7b) [13,33].

The initial standard-state entropy S^0 of $TBPH^+$ was only an estimation. To optimize this value, it was fitted to the available temperature-dependent data of the extraction of H_2SO_4 and H_3PO_4 by undiluted TBP (Fig. 9) and HNO_3 by 40 vol% TBP (Fig. 10) [37,46,50]. The optimized entropy of $TBPH^+$ can be found in Table 1. The temperature seems to have only a very limited effect on the extraction of HNO_3 and H_2SO_4, but significant differences in the extraction strength of H_3PO_4 are encountered. The introduction of a temperature-dependent MIDRANGE interaction parameter between TBP and H_3PO_4 was necessary to represent the temperature dependence of H_3PO_4 extraction in the thermodynamic model (Table 2).

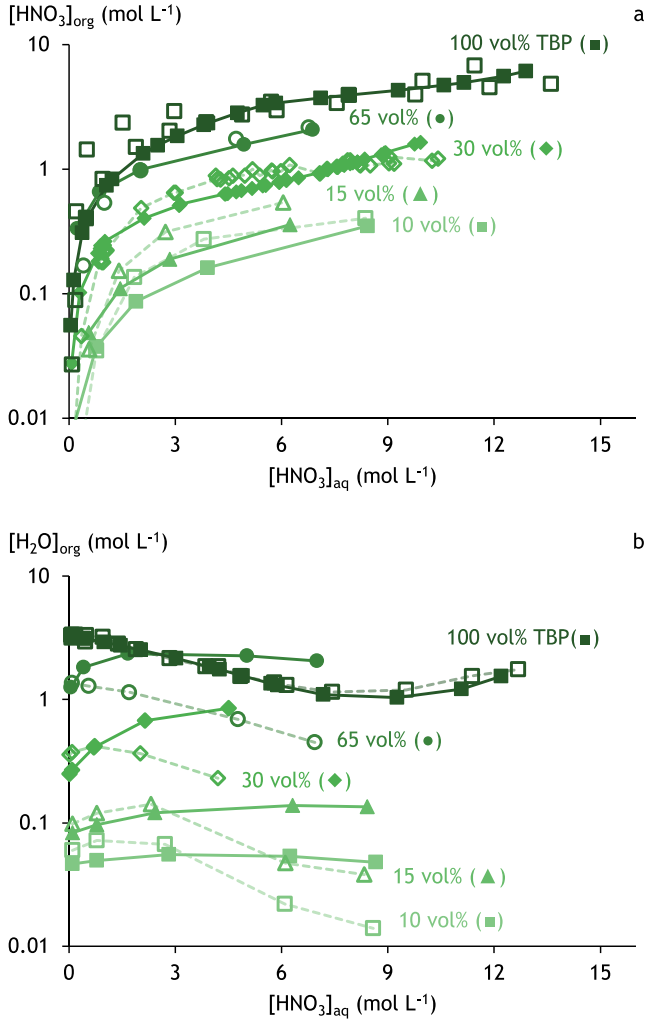

Fig. 7. Model fit (filled markers) to experimental data in HNO_3 systems of (a) the extraction of HNO_3 by, and (b) the solubility of water in, undiluted and diluted TBP (open markers) [13,33,35,47,50]. The labels show the TBP concentration in *n*-dodecane.

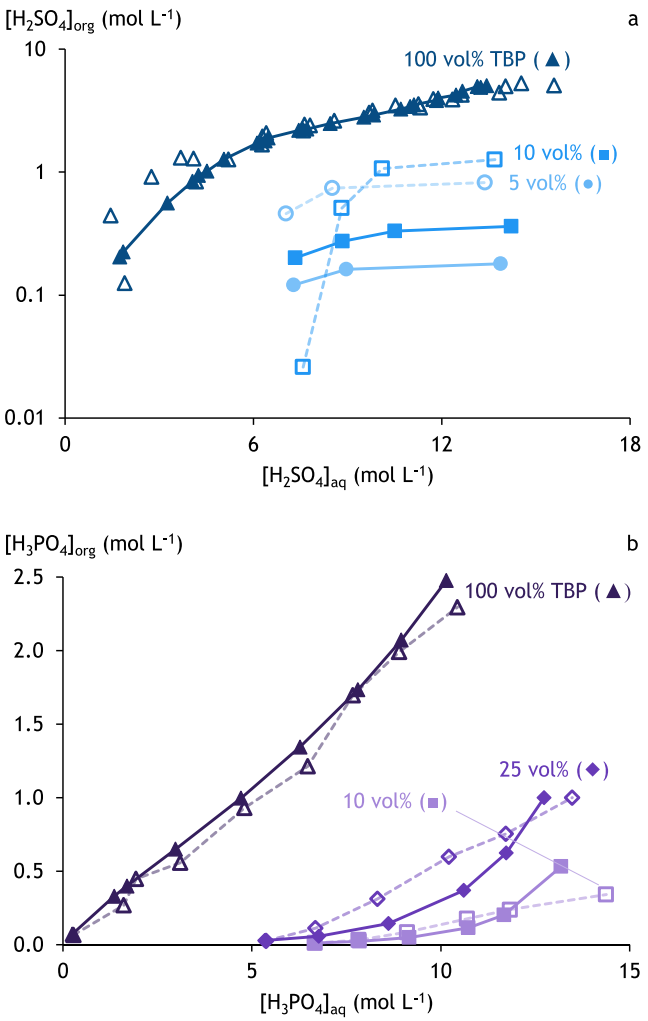

Fig. 8. Model fit (filled markers) to experimental data (open markers) of (a) the extraction of H_2SO_4, and (b) the extraction of H_3PO_4 by undiluted TBP and TBP in *n*-dodecane [36,37,45].

3.4. Overview of the thermodynamic model

The use of different literature sources for the extraction and water solubility data entails that the model cannot calculate all data points with perfect accuracy, because the results of these different literature sources are not always fully consistent. This happens because different experimental procedures and/or analytical techniques have been used. Nevertheless, the thermodynamic model is able to accurately fit the extraction of the modeled acids by TBP and the solubility of water in the organic over the entire range of relevant chemical conditions (Fig. 11).

The Gibbs energy of transfer ($\Delta G_{transfer}$) of an acid is more directly related to the underlying thermodynamics of the extraction process and the thermodynamic OLI-MSE model. Therefore, $\Delta G_{transfer}$ of the experimental data and model fits are also calculated for the most important graphs. The resulting graphs can be found in the Supporting Information (SI) to avoid cluttering the main text. More specifically, Fig. 4a is reproduced in energy terms to show the extraction from single-acid solutions by undiluted TBP. Fig. 6 is reproduced as an example of the extraction from multi-acid solutions. Fig. 7 is recalculated to show the effect of the diluent on the $\Delta G_{transfer}$ of HNO_3 and water, while Fig. 9 is recomputed in energy terms to show the effect of temperature.

In general, the $\Delta G_{transfer}$ are slightly positive, indicating a quite inefficient extraction of acids. Furthermore, the model fits in energy terms also agree well with the experimental data. Significant scatter of the experimental data is observed on the $\Delta G_{transfer}$ scale at low total acid

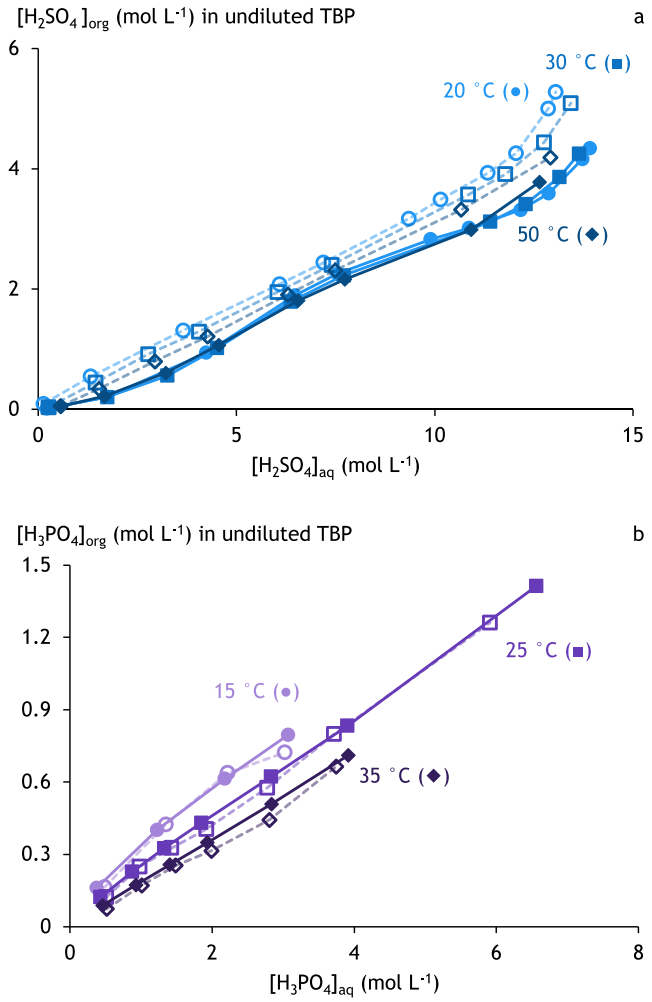

Fig. 9. Model fit (filled markers) to experimental data of the extraction of (a) H_2SO_4 and (b) H_3PO_4 (open markers) [37,46]. The labels show the equilibrium temperature.

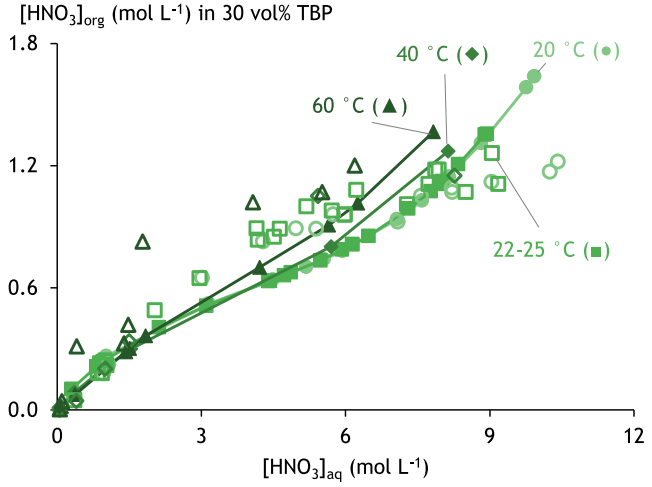

Fig. 10. Model fit (filled markers) to experimental data of the extraction of HNO_3 (open markers). The labels show the equilibrium temperature [35,50].

contents. This is probably related to significant experimental errors when only small absolute changes in acid concentrations are measured at these low total acid contents.

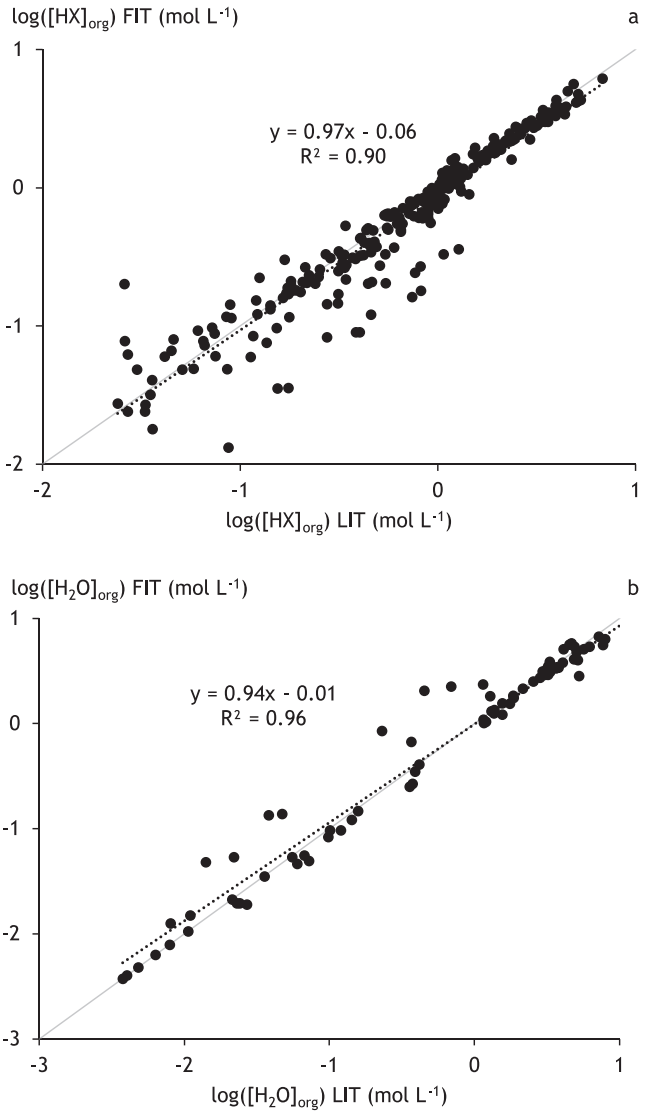

Fig. 11. Quality of fit graphs for (a) the extraction of acid, and (b) the solubility of water in the organic phase. The grey diagonal lines represent a perfect fit. LIT means literature data. The dotted lines are linear fits of the data with their details shown in the text next to the lines.

3.5. Non-reactive thermodynamic model

The addition of extra species to a thermodynamic model should be critically evaluated. One must refrain from introducing a new species that is only hypothetical in nature, and for which there exists no experimental evidence. This ensures a model is obtained with the highest chemical accuracy, and thus, prediction power. As mentioned earlier, the proton transfer of the strong mineral acids to TBP is documented in both experimental and quantum computational studies, but the existence of $TBPH^+$ species should not be taken for granted. To decide whether it is absolutely necessary to introduce the $TBPH^+$ species in the model, the construction of an alternative thermodynamic model was attempted. This alternative model, for clarity, termed the *non-reactive thermodynamic model*, is based on the distribution of protonated and deprotonated mineral acid to the organic phase. The extraction of deprotonated acid (Cl^-, NO_3^-, or HSO_4^-) also requires the stabilization of H_3O^+ in the organic phase. Thus, the following non-reactive solvent extraction equilibria can occur in the non-reactive thermodynamic model for a monoprotic acid (HX):

$$X^- + H_3O^+ \rightleftharpoons \overline{X^-} + \overline{H_3O^+} \quad (9)$$

$$HX \rightleftharpoons \overline{HX} \quad (10)$$

For clarity, the main thermodynamic model discussed in this paper, with the formation of $TBPH^+$, is a *reactive thermodynamic model*, where chemical bonds are formed during the extraction. Equation (9) does not occur in the reactive thermodynamic model and is replaced by:

$$HX + \overline{TBP} \rightleftharpoons \overline{X^-} + \overline{TBPH^+} \quad (11)$$

An overview of the non-reactive thermodynamic model is given in the SI, together with an extensive comparison of that model with the reactive thermodynamic model described in the main text. In summary, the non-reactive thermodynamic model is inferior to the reactive thermodynamic model. It is less accurate for the calculation of strong acids by undiluted TBP, and it fails to describe the extraction of strong acids by diluted TBP.

3.6. Model validation

The solvent extraction of H_3AsO_4 in strongly acidic media was added to the thermodynamic model to test whether the model can be extended without the need to change the already optimized thermodynamic values and binary interaction parameters. This is a verification of the generality of the current approach. H_3AsO_4 is a weak acid with three acid deprotonation constants (pKa_1, pKa_2, and pKa_3). These constants, and their temperature dependence, were optimized in the thermodynamic model by determining the ΔG_f^0 and S^0 values of H_3AsO_4 and its (partly) deprotonated species (Table 3). The data used to regress these values came from Perrin (Fig. 12a) [48]. Data on the water activity of H_3AsO_4 solutions were used to determine the H_2O–H_3AsO_4 binary interaction parameter, which is required to describe the behavior of H_3AsO_4 in the thermodynamic model at higher ionic strengths (Fig. 12b) [52].

Once the aqueous phase was optimized, the extraction of H_3AsO_4 could be modeled by optimizing the binary interaction parameters between $H_3AsO_4/H_2AsO_4^-$ and the extractant (Table 4). Interactions between $HAsO_4^{2-}/AsO_4^{3-}$ and the extractant were not necessary because these species do not form in acidic conditions. The complete extraction behavior of As(V) could be modeled using H_3AsO_4 solvent extraction data from Navarro and Alguacil [53], Jantunen *et al.* [54], and Demirkiran *et al.* [55]. An overview of the model fits can be found in Fig. 13 and Fig. 14. Extraction, scrubbing, and stripping data were used to determine the binary interaction parameters. These three steps in the solvent extraction process can be used together because they represent the same chemical equilibria. H_3AsO_4 extraction is strongly temperature-dependent (Fig. 13 c). This temperature dependence could be modeled by introducing a linear temperature dependence in the TBP–H_3AsO_4 UNIQUAC binary interaction parameter (Table 4).

The binary interaction parameters with H_2SO_4 or HSO_4^- were not altered because they were already optimized. This means that the H_2SO_4 extraction and the formation of $TBPH^+$ are predictions and not fittings. Both the H_3AsO_4 extraction fit and the H_2SO_4 extraction predictions are within 5 % error of the experimental data (Fig. 15).

Table 3
Standard-state thermodynamic properties of the relevant As(V) species, optimized in the thermodynamic model.

Species	ΔG_f^0 (kJ mol^{-1})	ΔH_f^0 (kJ mol^{-1})	S_f^0 (J mol^{-1} K^{-1})
H_3AsO_4	−767.1	−931.2	91.07
$H_2AsO_4^-$	−754.0	−894.5	105.0
$HAsO_4^{2-}$	−714.0	−864.0	7.621
AsO_4^{3-}	−646.6	−881.3	−341.6
As_2O_5 (s)[a]	−782.5		

[a] (s) means solid

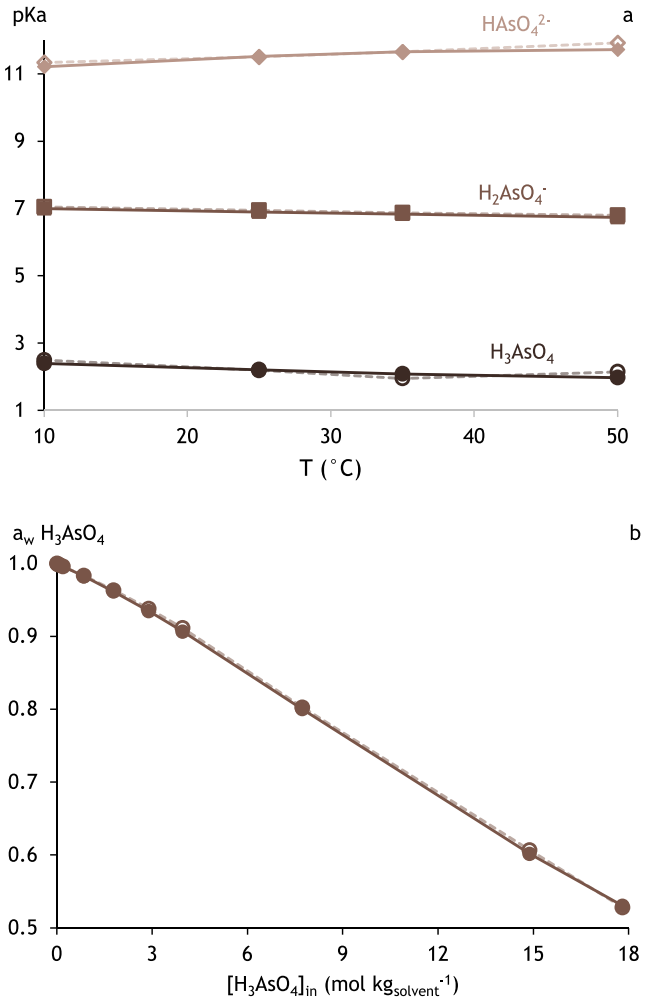

Fig. 12. Model fit (filled markers and solid lines) to the experimental (a) pKa values and (b) water activity of H_3PO_4 (open markers and dotted lines) [48,52].

Table 4
Extra UNIQUAC and MIDRANGE binary interaction parameters to calculate the extraction of HNO_3 from $Ca(NO_3)_2$ media, and As(V).

Species	UNIQUAC[a]		MIDRANGE[b]	
	a_{ij}	a_{ji}	b	c
H_2O–H_3AsO_4			2.9631	
TBP–H_3AsO_4 (0)	−13401[c]	10000[c]	−2.1766	
TBP–H_3AsO_4 (1)	19.519[c]			
TBP–$H_2AsO_4^-$			−2	
TBP–Ca^{2+} (2)			−7500[d]	

[a] UNIQUAC binary interaction parameters.
[b] MIDRANGE binary interaction parameters: $MR(ij) = b_{ij} + c_{ij} \bullet exp\left(-\sqrt{I+0.01}\right)$ with I the ionic strength of the solution.
[c] $a_{ij} = a(0)_{ij} + a(1)_{ij} \bullet T$ with T the absolute temperature in Kelvin.
[d] $b_{ij} = b(0)_{ij} + b(2)_{ij}/T$

Upon extraction of large amounts of acid and water, the volume of the undiluted TBP organic phase significantly increases, while the volume of the aqueous phase decreases. This non-negligible change in organic over aqueous ratio (O/A) is more pronounced when the initial O/A is higher. By defining the molar volume of TBP and $TBPH^+$ in the thermodynamic model (Table 1), it is possible to calculate the equilibrium volume of the organic phase starting from the initial number of moles or masses of the constituents of the aqueous and organic phases.

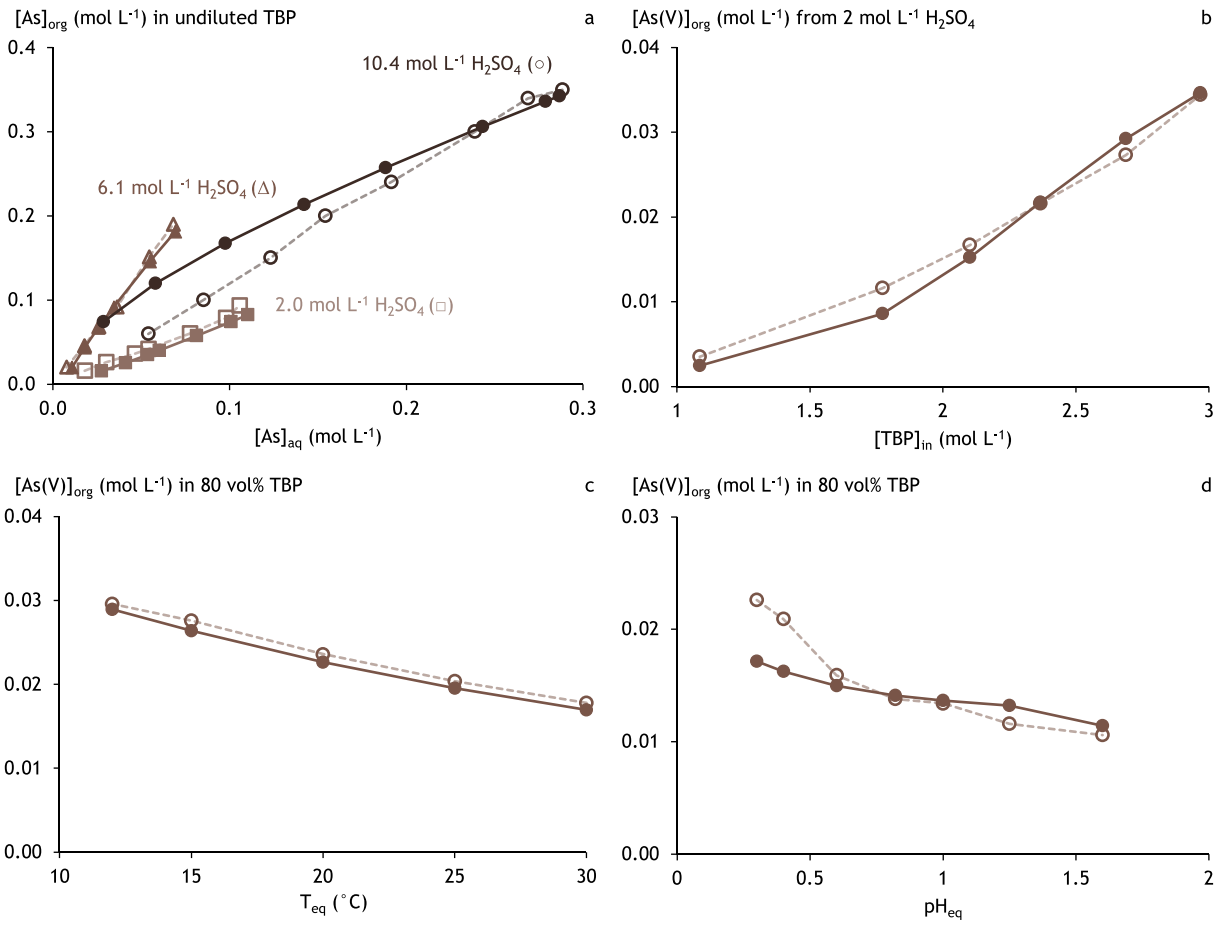

Fig. 13. Model fits (filled markers) to experimental H_3AsO_4 extraction data (open markers). (a) extraction isotherms from several initial H_2SO_4 concentrations (labels), (b) extractant dependence – 0.12 mol L^{-1} As(V) in the feed, (c) equilibrium temperature dependence – 0.1 mol L^{-1} As(V); 0.25 mol L^{-1} H_2SO_4, and (d) equilibrium pH dependence – 0.13 mol L^{-1} As(V) [53–55].

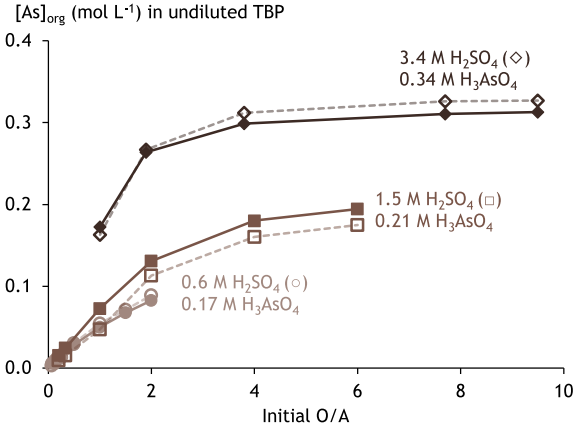

Fig. 14. Model fits (filled markers) to experimental H_3AsO_4 scrubbing and stripping data (open markers). The labels show the composition of the initial organic phase, with M representing mol/L.

The equilibrium volume of the aqueous phase is already accurately calculated because of the data present in the standard OLI-MSE database [20]. OLI uses the molar volume of water and binary interaction parameters between water and the most important solutes to obtain an accurate value for the density in the aqueous phase.

Data from Jantunen *et al.* on the relation between initial and equilibrium O/A were used to assess the accuracy of this volume calculation (Fig. 16) [54]. The results show that this simple approach of only adding the molar volume of TBP and $TBPH^+$ works very well for the calculation of densities and organic volume in acid extraction systems with TBP. Hence, the presented thermodynamic framework can be used in both units of amount and concentration.

Finally, the prediction capabilities of the thermodynamic model were validated by calculating the extraction of acids in mixed acids and salt/acid systems. This type of data was not used to determine the thermodynamic parameters in the model; hence the quality of these calculations reflects the model's extrapolation capabilities.

The first validation dataset comprises the extraction of HNO_3 from mixtures of aqueous HNO_3 and $Ca(NO_3)_2$ [46]. The behavior of Ca $(NO_3)_2$, Ca^{2+} and nitrate in Ca^{2+} media are accurately calculated in the aqueous phase because their thermodynamic data is available in the database from OLI. However, no binary interaction parameters between Ca^{2+} and TBP or other species that are related to the calculation of acid extraction by TBP are determined. Fig. 17 shows that the thermodynamic model can accurately predict the extraction of HNO_3 from mixed HNO_3–$Ca(NO_3)_2$ systems.

The second type of validation data relates to the extraction of acids from mixed-acid systems. One dataset includes the extraction of HCl and H_3PO_4 from 0.2 to 2.1-mol L^{-1} HCl, and 1.6 to 3.7 mol L^{-1} H_3PO_4 solutions [56], while the other handles the extraction of HNO_3 and H_3PO_4 from 0.2 to 4.0 mol L^{-1} HNO_3, 0 to 1 mol L^{-1} $Ca(NO_3)_2$, and 0 to 4 mol L^{-1} H_3PO_4 solutions [46]. All these extractions are performed with undiluted TBP at an initial O/A of 1. The predictions of the acid extractions in these datasets are well within ±10 % deviation from the experimental data (Fig. 18). This is within acceptable limits given the

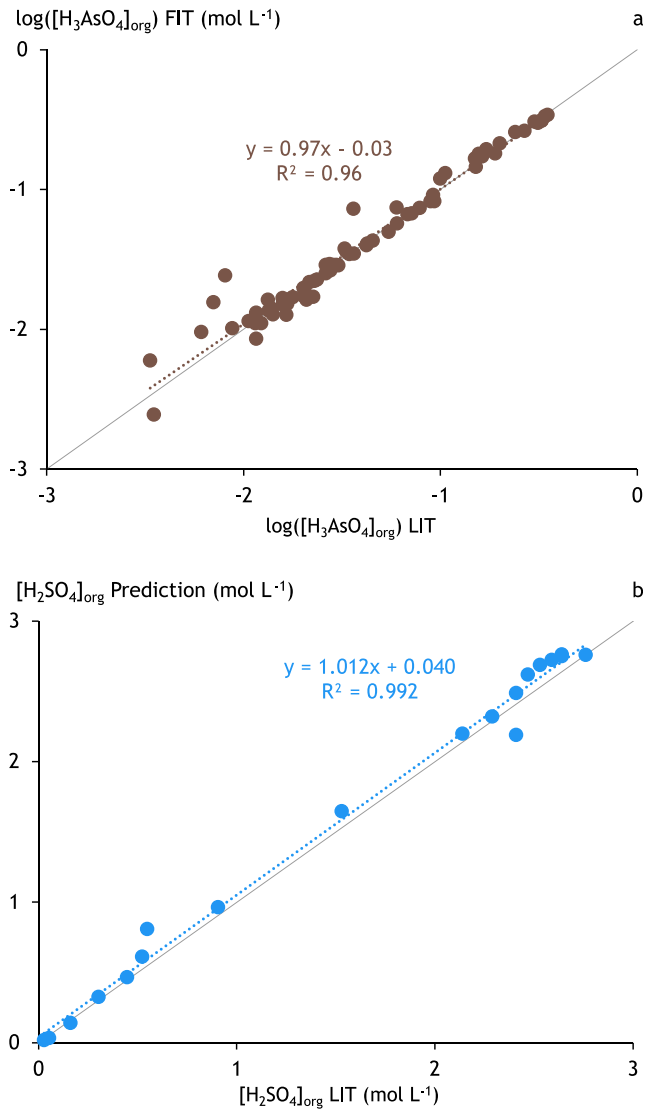

Fig. 15. (a) Quality of fit graph, and (b) quality of prediction graph for the H_3AsO_4–H_2SO_4 mixed acid data. LIT means literature data. The dotted lines are linear fits of the data.

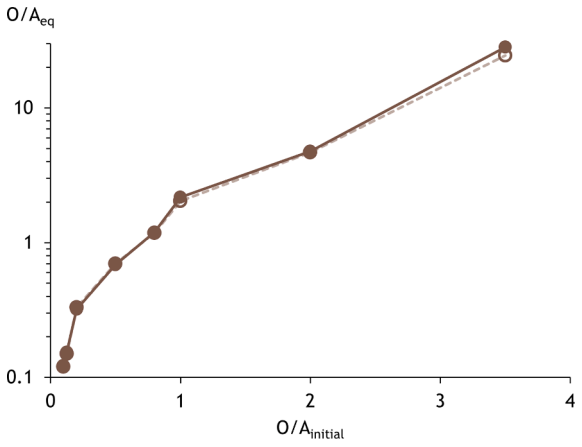

Fig. 16. Equilibrium organic over aqueous ratio (O/A) against initial O/A. The full markers represent the thermodynamic model prediction, while the open markers and dotted lines represent the experimental data [54].

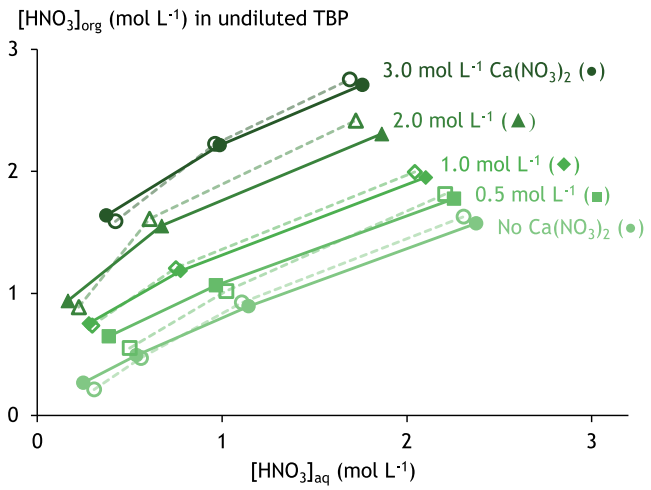

Fig. 17. Prediction (filled markers) of HNO_3 extraction from mixed HNO_3–$Ca(NO_3)_2$ systems (open markers) [46].

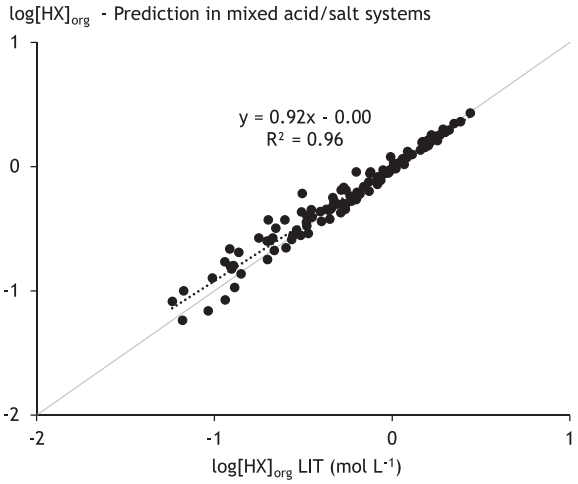

Fig. 18. Quality of the prediction of the acid extractions from mixed-acid solutions by undiluted TBP. The acids are HNO_3, HCl, and H_3PO_4. LIT means literature data. The dotted lines are linear fits of the data with their details shown in the text next to the lines.

variability in the experimental data between different sources. Also, note that the deviations tend to increase at lower acid concentrations. This is expected, given the larger relative experimental error when the measured concentration is lower. On the other hand, the extraction of acid from higher acid concentrations is almost perfectly predicted, with significantly less spread.

4. Conclusions

A semi-empirical molecular thermodynamic model was constructed that can be used to calculate the complete equilibrium of solvent extractions of HNO_3, HCl, H_2SO_4, H_3PO_4, and H_3AsO_4 by undiluted and diluted TBP between 10 and 60 °C. This model is based on one thermodynamic framework, the OLI Mixed-Solvent Electrolyte (OLI-MSE) framework, which describes the speciation of all compounds, the activity corrections in all phases, and the multi-phase equilibria. The extraction of mineral acids (HX) is universally described in this model by protonation of TBP to form the $TBPH^+$ species in the organic phase with coextraction of the mineral acid anion X^-. At very high mineral acid concentrations and for weak mineral acids, the extraction of neutral HX molecules can become dominant. The universality of this approach is

demonstrated by the accurate calculation of five different mineral acid extraction systems with the same thermodynamic framework and chemical model. The protonation of TBP by strong mineral acids is supported by literature data and by the inability to construct an accurate thermodynamic extraction model without the introduction of the $TBPH^+$ species. The predictive power and robustness of the presented modeling approach are supported by two different examples. First, the thermodynamic model is easily extended to calculate the extraction of a new mineral acid. Second, the extractions of acids from mixed-acid/salt systems are accurately predicted, while the model is mainly constructed using single-acid systems.

CRediT authorship contribution statement

Rayco Lommelen: Conceptualization, Methodology, Validation, Formal analysis, Investigation, Validation, Writing – original draft, Visualization. **Koen Binnemans:** Conceptualization, Writing – review & editing, Supervision, Resources, Funding acquisition.

Declaration of Competing Interest

The authors declare that they have no known competing financial interests or personal relationships that could have appeared to influence the work reported in this paper.

Data availability

Data will be made available on request.

Acknowledgements

This work was supported by the European Union's Framework Programme for Research and Innovation Horizon Europe [Grant number 101058124 (ENICON)]. The authors want to thank Jan Luyten and Joris Roosen (Umicore, Belgium) for the insightful discussions during the construction of the thermodynamic model.

Appendix A. Supplementary material

Supplementary data to this article can be found online at https://doi.org/10.1016/j.seppur.2023.123475.

References

[1] A. Agrawal, K.K. Sahu, An overview of the recovery of acid from spent acidic solutions from steel and electroplating industries, J. Hazard. Mater. 171 (2009) 61–75, https://doi.org/10.1016/j.jhazmat.2009.06.099.
[2] U. Kesieme, A. Chrysanthou, M. Catulli, C.Y. Cheng, A review of acid recovery from acidic mining waste solutions using solvent extraction, J. Chem. Technol. Biotechnol. 93 (2018) 3374–3385, https://doi.org/10.1002/jctb.5728.
[3] V.S. Kislik, Chapter 2 - Principles of Solvent Extraction of Organic and Mineral Acids, in: V.S. Kislik (Ed.), Solvent Extraction, Elsevier, Amsterdam, Amsterdam, 2012, pp. 69–111, https://doi.org/10.1016/B978-0-444-53778-2.10002-0.
[4] U.K. Kesieme, H. Aral, M. Duke, N. Milne, C.Y. Cheng, Recovery of sulphuric acid from waste and process solutions using solvent extraction, Hydrometallurgy. 138 (2013) 14–20, https://doi.org/10.1016/j.hydromet.2013.06.005.
[5] R.-S. Juang, R.-H. Huang, R.-T. Wu, Separation of citric and lactic acids in aqueous solutions by solvent extraction and liquid membrane processes, J. Membr. Sci. 136 (1997) 89–99, https://doi.org/10.1016/S0376-7388(97)00176-2.
[6] J. Rydberg, M. Cox, C. Musikas, G.R. Choppin, Solvent extraction principles and practice, revised and expanded, 2nd ed., Marcel Dekker, New York, New York, 2004.
[7] M. Wang, Y. Yu, C.C. Chen, Modeling mixed-solvent electrolyte systems, Chem. Eng. Prog. 112 (2016) 34–42.
[8] S. Dash, S. Mohanty, Mathematical modeling aspect in solvent extraction of metals, Sep. Purif. Rev. 50 (2021) 74–95, https://doi.org/10.1080/15422119.2019.1648294.
[9] H. Chen, A.J. Masters, R. Taylor, M. Jobson, D. Woodhead, Application of SAFT-VRE in the flowsheet simulation of an advanced PUREX process, Ind. Eng. Chem. Res. 58 (2019) 3822–3831, https://doi.org/10.1021/acs.iecr.8b05606.
[10] S. Balasubramonian, N.K. Pandey, R.V. Subba Rao, Comparison of activity coefficient models for the estimation of uranyl nitrate and nitric acid distribution coefficients in phosphoric solvent, Prog. Nucl. Energy. 128 (2020), 103472, https://doi.org/10.1016/j.pnucene.2020.103472.
[11] E.A. Puzikov, B.Y. Zilberman, Y.S. Fedorov, I.V. Blazheva, A.S. Kudinov, N. D. Goletskiy, D.V. Ryabkov, A new approach to simulation of extraction equilibria in the PUREX process, Solvent Extr. Ion Exch. 33 (2015) 362–384, https://doi.org/10.1080/07366299.2014.993238.
[12] B. Tan, C. Chang, D. Xu, Y. Wang, T. Qi, Modeling of the competition between uranyl nitrate and nitric acid upon extraction with Tri-n-butyl phosphate, ACS Omega. 5 (2020) 12174–12183, https://doi.org/10.1021/acsomega.0c00583.
[13] E.A. Puzikov, B.Y. Zilberman, A.S. Kudinov, N.D. Goletskii, Description of the extraction of trivalent REE and TPE nitrates with tributyl phosphate and its solutions in paraffins in the presence of nitric acid and salting-out agents using a unified model, Radiochemistry. 61 (2019) 689–693, https://doi.org/10.1134/S1066362219060080.
[14] A. Chagnes, Simulation of solvent extraction flowsheets by a global model combining physicochemical and engineering approaches—application to cobalt(II) extraction by D2EHPA, Solvent Extr. Ion Exch. 38 (2020) 3–13, https://doi.org/10.1080/07366299.2019.1691135.
[15] C.F. Baes Jr., Modeling Solvent Extraction Systems with SXFIT, Solvent Extr. Ion Exch. 19 (2001) 193–213, https://doi.org/10.1081/SEI-100102691.
[16] L. Cohen, T. McCallum, O. Tinkler, W. Szolga, Technological Advances, Challenges and Opportunities in Solvent Extraction from Energy Storage Applications, in: Extraction 2018: The Minerals, Metals & Materials Series, 2018: pp. 2033–2045, doi: 10.1007/978-3-319-95022-8_170.
[17] C.O. Iloeje, F. Carlos, J. Jové Colón, D.J.G. Cresko, Gibbs energy minimization model for solvent extraction with application to rare-earths recovery, Environ. Sci. Technol. 53 (2019) 7736–7745, https://doi.org/10.1021/acs.est.9b01718.
[18] J. Prausnitz, R. Lichtenthaler, E.G. de Azevedo, Molecular thermodynamics of fluid-phase equilibria, 3rd ed., Pearson, Upper Saddle River NJ, Upper Saddle River, N.J., 1998.
[19] A. Klamt, The COSMO and COSMO-RS solvation models, WIREs Comput. Mol. Sci. 8 (2018) e1338.
[20] P. Wang, A. Anderko, R.D. Young, A speciation-based model for mixed-solvent electrolyte systems, Fluid Phase Equilib. 203 (2002) 141–176, https://doi.org/10.1016/S0378-3812(02)00178-4.
[21] P. Wang, A. Anderko, R.D. Springer, R.D. Young, Modeling phase equilibria and speciation in mixed-solvent electrolyte systems: II. Liquid–liquid equilibria and properties of associating electrolyte solutions, J. Mol. Liq. 125 (2006) 37–44, https://doi.org/10.1016/j.molliq.2005.11.030.
[22] J.E. Hoffmann, The purification of copper refinery electrolyte, JOM 56 (2004) 30–33, https://doi.org/10.1007/s11837-004-0088-4.
[23] H. Su, Z. Li, J. Zhang, W. Liu, Z. Zhu, L. Wang, T. Qi, Combining selective extraction and easy stripping of lithium using a ternary synergistic solvent extraction system through regulation of Fe^{3+} Coordination, ACS Sustain. Chem. Eng. 8 (2020) 1971–1979, https://doi.org/10.1021/acssuschemeng.9b06432.
[24] L. Pietrelli, S. Ferro, M. Vocciante, Raw materials recovery from spent hydrochloric acid-based galvanizing wastewater, Chem. Eng. J. 341 (2018) 539–546, https://doi.org/10.1016/j.cej.2018.02.041.
[25] L. Cui, L. Wang, M. Feng, L. Fang, Y. Guo, F. Cheng, Ion-pair induced solvent extraction of lithium (I) from acidic chloride solutions with tributyl phosphate, Green, Energy Environ. 6 (2021) 607–616, https://doi.org/10.1016/j.gee.2020.05.002.
[26] A.B. Botelho Junior, D.C.R. Espinosa, J.A.S. Tenório, Selective separation of Sc(III) and Zr(IV) from the leaching of bauxite residue using trialkylphosphine acids, tertiary amine, tri-butyl phosphate and their mixtures, Sep. Purif. Technol. 279 (2021), 119798, https://doi.org/10.1016/j.seppur.2021.119798.
[27] D.S. Abrams, J.M. Prausnitz, Statistical thermodynamics of liquid mixtures: A new expression for the excess Gibbs energy of partly or completely miscible systems, AIChE J. 21 (1975) 116–128, https://doi.org/10.1002/aic.690210115.
[28] P. Wang, A. Anderko, Computation of dielectric constants of solvent mixtures and electrolyte solutions, Fluid Phase Equilibria. 186 (2001) 103–122, https://doi.org/10.1016/S0378-3812(01)00507-6.
[29] R. Lommelen, K. Binnemans, Thermodynamic modeling of salting effects in solvent extraction of cobalt(II) from chloride media by the basic extractant methyltrioctylammonium chloride, ACS Omega. 6 (2021) 11355–11366, https://doi.org/10.1021/acsomega.1c00340.
[30] D. Bourgeois, A. El Maangar, S. Dourdain, Importance of weak interactions in the formulation of organic phases for efficient L/L extraction of metals, Curr. Opin. Colloid Interface Sci. 46 (2020) 36–51, https://doi.org/10.1016/j.cocis.2020.03.004.
[31] M. Špadina, S. Dourdain, J. Rey, K. Bohinc, S. Pellet-Rostaing, J.-F. Dufrêche, T. Zemb, How acidity rules synergism and antagonism in liquid–liquid extraction by lipophilic extractants—Part II: Application of the ienaic modelling, Solvent Extr. Ion Exch. 40 (2022) 106–139, https://doi.org/10.1080/07366299.2021.1899614.
[32] S. Gourdin-Bertin, J.-F. Dufrêche, M. Duvail, T. Zemb, Microemulsion as model to predict free energy of transfer of electrolyte in solvent extraction, Solvent Extr. Ion Exch. 40 (2022) 28–63, https://doi.org/10.1080/07366299.2021.1953259.
[33] E. Hesford, H.A.C. McKay, The extraction of mineral acids by tri-n-butyl phosphate (TBP), J. Inorg. Nucl. Chem. 13 (1960) 156–164, https://doi.org/10.1016/0022-1902(60)80248-5.
[34] A.S. Kertes, Solute-solvent interaction in the system hydrochloric acid-water-tri-n-butyl phosphate, J. Inorg. Nucl. Chem. 14 (1960) 104–113, https://doi.org/10.1016/0022-1902(60)80206-0.
[35] C.F.J. Colón, H.K. Moffat, R.R. Rao, Modeling of liquid-liquid extraction (LLE) equilibria using gibbs energy minimization (GEM) for the system

TBP–HNO_3–UO_2–H_2O–Diluent, Solvent Extr. Ion Exch. 31 (2013) 634–651, https://doi.org/10.1080/00397911.2013.785882.
[36] E. Brauer, E. Högfeldt, On the extraction of water from sulphuric acid solutions into tri-n-butyl phosphate, J. Inorg. Nucl. Chem. 23 (1961) 115–121, https://doi.org/10.1016/0022-1902(61)80091-2.
[37] C. Hanson, A.N. Patel, Distribution of sulphuric acid between tri-n-butyl phosphate and water, J. Appl. Chem. 19 (1969) 20–24, https://doi.org/10.1002/jctb.5010190106.
[38] A. Apelblat, Extraction of sulphuric acid by methyl diphenyl phosphate and tributyl phosphate, J. Chem. Soc., Dalton Trans. (1973) 1198–1201, https://doi.org/10.1039/DT9730001198.
[39] L. Azéma, S. Ladame, C. Lapeyre, A. Zwick, F. Lakhdar-Ghazal, Does phosphoryl protonation occurs in aqueous phosphoesters solutions, Spectrochim. Acta, Part A 62 (2005) 287–292, https://doi.org/10.1016/j.saa.2004.12.038.
[40] M. Baaden, M. Burgard, G. Wipff, TBP at the water−oil interface: The effect of TBP concentration and water acidity investigated by molecular dynamics simulations, J. Phys. Chem. B. 105 (2001) 11131–11141, https://doi.org/10.1021/jp011890n.
[41] A. Dhawa, A. Rout, N.R. Jawahar, K.A. Venkatesan, A systematic approach for achieving the maximum loading of Eu(III) in TODGA/n-dodecane phase with the aid of TBP phase modifier, J. Mol. Liq. 341 (2021), 117397, https://doi.org/10.1016/j.molliq.2021.117397.
[42] H. Su, Z. Li, Z. Zhu, L. Wang, T. Qi, Extraction relationship of Li^+ and H^+ using tributyl phosphate in the presence of Fe(III), Sep. Sci. Technol. 55 (2020) 1677–1685, https://doi.org/10.1080/01496395.2019.1604759.
[43] P. Velavendan, S. Ganesh, N.K. Pandey, R. Geetha, M.K. Ahmed, U. Kamachi Mudali, R. Natarajan, Studies on solubility of TBP in aqueous solutions of fuel reprocessing, J. Radioanal. Nucl. Chem. 295 (2013) 1113–1117, https://doi.org/10.1007/s10967-012-1945-1.
[44] K. Ziat, B. Mesnaoui, T. Bounahmidi, R. Boussen, M. de la Guardia, S. Garrigues, Modelling of the ternary system H_3PO_4/H_2O/TBP, Fluid Phase Equilibria. 201 (2002) 259–267, https://doi.org/10.1016/S0378-3812(02)00134-6.
[45] R. Dhouib-Sahnoun, M. Feki, H.F. Ayedi, Liquid−liquid equilibria of the ternary system water + phosphoric acid + tributyl phosphate at 298.15 K and 323.15 K, J. Chem. Eng. Data. 47 (2002) 861–866, https://doi.org/10.1021/je010293r.
[46] Y. Zhang, M. Valiente, M. Muhammed, Extraction of nitric and phosphoric acids with tributyl phosphate, Solvent Extr. Ion Exch. 7 (1989) 173–200, https://doi.org/10.1080/07360298908962304.
[47] D.F. Peppard, G.W. Mason, J.L. Maier, Interrelationships in the solvent extraction behaviour of scandium, thorium, and zirconium in certain tributyl phosphate-mineral acid systems, J. Inorg. Nucl. Chem. 3 (1956) 215–228, https://doi.org/10.1016/0022-1902(56)80022-5.
[48] D.D. Perrin, Dissociation contants of inorganic acids and bases in aqueous solution, Pure Appl. Chem. 20 (1969) 133–236, https://doi.org/10.1351/pac196920020133.
[49] C. Liu, J. Cao, W. Shen, Y. Ren, W. Mu, X. Ding, Liquid – liquid equilibria of quaternary system phosphoric acid/sulfuric acid/water/tri-n-butyl phosphate and the formation of extraction complex at 303.2 K, Fluid Phase Equilib. 408 (2016) 190–195, https://doi.org/10.1016/j.fluid.2015.09.015.
[50] G. Petrich, Z. Kolarik, The 1981 purex distribution data index, Kernforschungszentrum Karlsruhe, Germany, 1981.
[51] D.F. Haghshenas, D. Darvishi, H. Rafieipour, E.K. Alamdari, A.A. Salardini, A comparison between TEHA and Cyanex 923 on the separation and the recovery of sulfuric acid from aqueous solutions, Hydrometallurgy. 97 (2009) 173–179, https://doi.org/10.1016/j.hydromet.2009.02.006.
[52] H. Yang, Q. Wang, Q. Zhou, J. Yue, Isopiestic measurements of water activities for an arsenic acid aqueous solution at 298.15 K, J. Chem. Eng. Data. 62 (2017) 3306–3312, https://doi.org/10.1021/acs.jced.7b00349.
[53] P. Navarro, F.J. Alguacil, Removal of arsenic from copper electrolytes by solvent extraction with tributylphosphate, Can. Metall. Q. 35 (1996) 133–141, https://doi.org/10.1179/cmq.1996.35.2.133.
[54] N. Jantunen, S. Virolainen, P. Latostenmaa, J. Salminen, M. Haapalainen, T. Sainio, Removal and recovery of arsenic from concentrated sulfuric acid by solvent extraction, Hydrometallurgy. 187 (2019) 101–112, https://doi.org/10.1016/j.hydromet.2019.05.008.
[55] A. Demirkiran, N.M. Rice, R. Wright, The Extraction of Arsenic(V) and Sulphuric Acid from Acidic Sulphate Media by Tri-n-butyl Phosphate (TBP) in Shellsol A or T: I - an Equilibrium Study, in: Proceedings of the International Solvent Extraction Conference, Johannesburg, 2002.
[56] C. Liu, Y. Ren, D. Tian, X. Zhang, Y. Wang, L. Kong, W. Shen, Equilibria of the quaternary system including phosphoric acid, hydrochloric acid, water and tri-n-butyl phosphate at T = 303.2 K and atmosphere pressure, J. Chem. Thermodyn. 79 (2014) 118–123, https://doi.org/10.1016/j.jct.2014.08.003.